

# The mixing of bubbles in two-dimensional bidisperse foams under extensional shear

S.J. Cox

*Institute of Mathematical and Physical Sciences and  
University of Wales Institute of Non-Newtonian Fluid Mechanics,  
University of Wales Aberystwyth, Ceredigion SY23 3BZ, UK.*

---

## Abstract

Two-dimensional bidisperse foams were simulated in cyclic, uniaxial, extensional shear. Mixing of bubbles of different sizes only occurs at high strains, and once mixed, the bubbles do not segregate. For liquid fractions up to 1%, the rate of mixing is shown to be slightly enhanced by increased liquid fraction.

*Key words:* Foam, Topological Changes, Mixing, Rheology, Surface Evolver

---

## 1 Introduction

The flow of foams is seen in many processes, and its use in major industries means that an understanding of the rheology of foams is of paramount importance [1, 2]. Although foams are disordered materials, they have well-defined equilibrium laws which allow their static structure to be determined. It is perhaps the combination of industrial importance with an attractive and precise local structure that makes foams one of the best candidates to improve the understanding of the rheology of multiphase fluids.

Foams are by nature opaque. While it is possible to perform three-dimensional experiments [3] and simulations [4] to understand the rheology of foam, as in many other fields much can be gained from considering a two-dimensional (2D) foam, such as can be made by trapping bubbles between two parallel and closely spaced

horizontal glass plates. Then each bubble can be seen, and its position tracked over time. Indeed, a large part of the recent literature attests to the profitability of such an approach, both experimentally [5, 6, 7, 8, 9], theoretically [10, 11] and computationally [12, 13, 14, 15].

In equilibrium, the idealized 2D foam used for computation consists of films which appear as circular arcs that meet three-fold at  $120^\circ$ . This is a consequence of the fact that the most important contribution to the energy of a film is its area, or, in 2D, its length [16, 17]. For the same reason, films meet solid boundaries at  $90^\circ$ . Thus, the search for the equilibrium structure of a 2D foam is equivalent to the problem of finding the least perimeter of a collection of circular arcs subject to area constraints (the bubbles). This is a problem admirably tackled by the Surface Evolver [18], and that software is employed here.

As is well-known, foams are elastic solids at low strain. They deform plastically as the strain increases until they act as liquids at high stress, above a so-called yield stress. We concentrate here on the plastic events that occur in a foam undergoing extensional shear. These plastic events take the form of local neighbour-switching topological changes, as illustrated in figure 1. As one film shrinks to zero length, an unstable four-fold vertex is formed. The Surface Evolver allows this vertex to be “popped”, so that the film can re-form with different neighbours, thus reducing the energy of the foam. These T1 topological transformations [19] thus provide a mechanism for dissipation in the quasi-static or zero shear-rate regime [20]. They also allow bubbles to change their positions relative to each other.

Whether a few topological changes can be said to have pushed a foam beyond its yield stress is a moot point, but undoubtedly the effect of these local changes is to allow a foam to reduce its energy and therefore to change its properties. Although the static shear-modulus of a foam does not depend greatly on its precise structure, it does depend upon bubble size [2]. In a polydisperse foam, the mixing or segregation of bubbles according to their size can therefore lead to regions of the foam with different responses to shear.

The liquid fraction  $\Phi_l$  of a 2D foam is defined as the ratio of liquid area to total area. The usual picture used for computation is that of a dry foam, but as liquid is added to the foam, the three-fold junctions swell, to form Plateau borders, as shown in

figure 2. This decoration of the structure [21] with small triangular liquid elements does not, however, provide the most easily accomplished method of simulating a wet foam. The effect of the liquid is to allow the T1 changes to occur at a vertex separation greater than the dry case predicts. We therefore introduce a critical cut-off length  $l_c$  which is applied to a dry foam to mimic a wet one:  $l_c$  represents the vertex separation at which T1s are triggered in the Surface Evolver simulations. Small  $l_c$  corresponds to dry foams, and increasing  $l_c$  to foams of greater liquid fraction. A geometrical calculation shows that

$$\Phi_l = 0.242 \frac{l_c^2}{\bar{A}} \quad (1)$$

where  $\bar{A}$  is the average bubble area. This method cannot be expected to be accurate for significantly wet foams; it is probably effective for foams of liquid fraction up to about 5%, when four-sided Plateau borders start to appear in the foam [20] and the decoration theorem fails [21].

The most simple 2D system in which to examine bubble sorting or mixing according to size is a bidisperse foam, in which a bubble has one of only two possible areas. Questions about whether sorted or mixed configurations of bubbles of two different sizes represent the minimum energy state have been addressed by Teixeira et al. [22]. They show that for a configuration in which the ratio of bubble areas is 2, as considered here, the least energy configuration is a sorted collection of ordered hexagons.

This paper explores whether such arrangements are stable under the application of cyclic extensional shear to the foam, or conversely, whether the shear can induce an optimal ordering. That is, does an initially sorted foam remain sorted, or can a mixed foam be sorted under shear? Shearing a foam may allow it to explore different arrangements of bubbles and to choose lower energy ones. The simulations are applied to disordered foams in a quasi-static fashion: a small increment in strain is followed by relaxation to a local minimum of film length, so that the foam moves through a series of equilibrium states in which Plateau's laws apply. During each step, many neighbour-switching T1 transformations may occur, although their precise order of occurrence is not resolved. However, even at this level of description, there are interesting effects, before details such as viscous drag are introduced. In-

deed, the introduction of viscous effects may reduce the amount of mixing.

## 2 Numerical implementation

All foams considered here consist of 100 bubbles in a square box that has initial width  $W_0 = 10$  and height  $H_0 = 10$ . A foam of this size is large enough for the effects of size-sorting to be seen, but not so large as to make simulations so slow as to be un-viable. The Surface Evolver works in dimensionless units, and since the only energy is proportional to the surface tension, its value is not important: we take it to be equal to one.

The foams are bidisperse: each bubble is assigned a target area of either  $A_b \approx 0.66$  or  $2A_b$ , with a roughly 50% probability, so that the average bubble area is one. From the initial state, the foam is deformed quasi-statically by increasing the strain  $\epsilon$  sinusoidally. Time is increased in steps of  $dt = 0.005$ , and at each step the foam is relaxed to equilibrium, with T1s being performed when a film shrinks below a critical length  $l_c$ . The dimensions of the rectangular box vary according to

$$W = W_0 e^{\epsilon_{max} \sin(t)}; \quad H = W_0 H_0 / W, \quad (2)$$

where  $\epsilon_{max}$  is the maximum strain reached. The strain is therefore area-preserving, and  $\epsilon_{max} = 1$  corresponds to  $W = 27.18$ ,  $H = 3.68$ .

In each of the simulations described below, five cycles of extension are simulated, so that time  $t$  lies in the range  $[0, 10\pi]$ . We commence with a small value of  $l_c = 0.01$ , which represents a very dry foam. The value of  $\epsilon_{max}$  is varied, and three different bubble distributions are investigated.

## 3 Sorting and mixing

To determine whether bubbles mix under shear, the starting configuration is one in which the large bubbles are all in the lower part of the box. This is referred to as foam 1, shown in figure 3(a). A small value of  $l_c = 0.01$  is chosen, which represents

a dry foam ( $\Phi_l \approx 2.42 \times 10^{-5}$ ). The effect of mixing is measured by counting the number of films that separate large from small bubbles,  $N_{sl}$ . The normal stress difference  $\tau_{xx} - \tau_{yy}$  is calculated by integrating the normal vector to each film along its length and resolving in  $x$  and  $y$  directions, then averaging over the whole foam. This allows a shear modulus to be found.

To ensure that the results for mixing are not affected by the initial strain being parallel to the interface between large and small bubbles, a second foam is simulated in which the large bubbles are initially on the left-hand side of the foam as in figure 3(b). Finally, to investigate if sorting occurs, a third set of simulations commence from a mixed foam, figure 3(c).

### 3.1 Results

Figure 4 quantifies the amount of mixing that occurs in the three foams. For low amplitude strains,  $\epsilon_{max} = 0.1$ , there is no change in the structure, hence  $N_{sl}$  is constant in this elastic regime. For  $\epsilon_{max} = 0.5$  there is a small cyclic variation in  $N_{sl}$  for each foam, but as the third row of figure 3 makes clear, there is no mixing in foam 1 or 2. At  $\epsilon_{max} = 0.75$  there is a definite relative motion of the small bubbles, but they mostly remain together. At high strain there is significant relative bubble motion, although for foam 3  $N_{sl}$  decreases only slightly from a value of about 130. Mixing occurs for both foams 1 and 2, where  $N_{sl}$  rises from a value of 19 to a value around 70 to 80 after 5 cycles. The results for foams 1 and 2 are qualitatively similar, showing that the orientation of the initial foam does not play a significant role.

The value of  $N_{sl}$  for foams 1 and 2 might be expected to saturate close to the value for foam 3. To test this assertion, foams 1 and 3 were simulated for 5 further strain cycles at  $\epsilon_{max} = 1.0$ , shown in figure 5. It is indeed the case that for both foams the degree of mixing tends to the same limit,  $N_{sl} \approx 90$ .

For mixing to occur, therefore, the maximum strain amplitude must be large (figure 8). This forces the small bubbles to be pushed out of the centre of the short side, so that in the next cycle they are redistributed (figure 9). At this large strain amplitude, the small decrease of  $N_{sl}$  in foam 3 may represent small bubbles moving preferen-

tially to the wall, at which point one of their sides does not count towards the total. Counting the peripheral bubbles in figure 3 shows that the number of bubbles, both large and small, touching the walls increases slightly at large amplitude strains for all three foams. In addition, the decrease of  $N_{sl}$  may denote a degree of sorting in foam 3, although it seems unlikely that this is a trend that would continue much further. A second simulation of an initially mixed foam was performed (data not shown), verifying that this behaviour is robust.

To justify simulating foams of only 100 bubbles, figure 6 compares the value of  $N_{sl}$  after 5 strain cycles with that in foams of larger size, up to 400 bubbles, for a range of values of the maximum strain  $\epsilon_{max}$ . When  $N_{sl}$  is scaled by the total number of bubbles, the results are indistinguishable.

Figure 7 shows how the stress evolves with strain. For small amplitude strains ( $\epsilon_{max} = 0.1$ ) the stress increases and decreases linearly, representing purely elastic behaviour, visible as a straight line through the origin. At higher strains, plastic events begin to occur, as films shrink to zero length and T1s are triggered. These events are visible as sudden drops in stress, which almost all occur as the width or height approaches its maximum value,

In all cases however, the shear modulus, measured as the slope of the stress-strain curve in the elastic regime on figure 7, is close to the value for the hexagonal honeycomb [2]. (This is no longer the case once the liquid fraction is greater than about 5% [20].)

As  $\Phi_l$  increases, however, there are more T1s. So increasing the liquid fraction results in faster mixing of the bubbles, even within this 5% limit, as shown in figure 10. The data is for foams 1 and 2, and the liquid fraction is increased by a factor of 25 ( $l_c$  increases from 0.01, the value used above, to 0.05). It is therefore clear that a wetter foam imparts greater mobility to the bubbles.

The maximum stress that the foam reaches in figure 7 is a measure of the yield stress  $\tau_s$  of the foam. For values of  $l_c$  between 0.001 and 0.2 (6 points), that is liquid fractions up to 1%, we fit the stress to a sinusoid

$$\tau_{xx} - \tau_{yy} = \tau_s \sin(t/t_0). \quad (3)$$

The values of  $\tau_s$  are then fitted to the square-root power law of Hutzler et al. [20]:

$$\frac{1}{2}\tau_s = a - b\sqrt{\Phi_l}, \quad (4)$$

giving  $a = 0.76 \pm 0.01$  and  $b = 3.17 \pm 0.16$ . This compares well with their fitted parameters,  $a = 0.74$ ,  $b = 3.4$ , despite the difference in boundary conditions and treatment of wet foam. That is, the simulations presented here treat a foam in a finite box, rather than one with periodic boundary conditions. Moreover, the PLAT software used by Hutzler et al. [20] explicitly includes the triangular Plateau borders; the agreement in values of the yield stress thus validates our use of a cut-off length to make the simulations more straightforward.

#### 4 Conclusions

The mixing of bubbles in bidisperse foams in extensional shear occurs only at high strains. Once mixed, the bubbles of different sizes do not segregate. For liquid fractions up to 1%, the rate of mixing is slightly enhanced by increased liquid fraction. The experiments of Quilliet et al. [9] show that when a monodisperse foam containing a single large bubble is sheared transversely, the large bubble moves towards the walls of the box. These simulations of extensional shear may be able to explain this observation – there is certainly an increase in the number of bubbles touching the wall in a mixed foam.

Indeed, the complementary experiment to the extensional shear presented here would be of great interest in validating these results. The means by which such an experiment could be accomplished are not immediately clear. The easiest may be to use a bubble raft, in which the foam floats above a liquid pool, or to enclose a bubble raft beneath a glass plate, as in [9]. These approaches suffer, however, from the foam having a high liquid fraction. To reach the dry limit, the foam may be trapped between glass plates; it is then difficult to manipulate the boundaries of the rectangular box smoothly, and in such a way as to preserve area. Perhaps the best approach might be to surround the foam, along with four small magnets at the corners, with an elastic membrane rather than rigid walls. The magnets could then be manipulated from outside the glass plates to drive the shear.

The effects of system size have not been discussed here. Preliminary simulations of foams with up to 400 bubbles show similar trends to those described here, with a slight increase in mixing at lower maximum strains. In addition to larger systems, future work will include the use of periodic boundary conditions to ascertain the effect, if any, of the solid boundaries used here.

As first described by Fullman [23], viscous effects may be introduced into the dry foam model by considering the drag as the liquid surfaces move along the bounding surfaces of the experiment. Both the vertex model [13, 14], in which the dissipation is concentrated at the vertices, and the recent model of Kern et al. [15], in which the dissipation occurs in the films while full structural information is retained, improve upon the usual quasi-static model of flow. The order in which T1 changes happen is also resolved. The precise effects that viscous drag has on bubble mixing and sorting remain to be seen.

## Acknowledgements

This work benefited from discussion with B. Dollet, F. Graner and P. McGuinness. D.H. Evans provided computer support. I acknowledge financial support from the Gooding Fund of the University of Wales Aberystwyth which enabled me to attend the UWNNFM Conference on Extensional Flow.

## References

- [1] A.M. Kraynik. 1988 Foam flows. *Ann. Rev. Fluid Mech.* **20**:325–357.
- [2] D. Weaire and S. Hutzler. 1999 *The Physics of Foams*. Clarendon Press, Oxford.
- [3] C. Monnereau and M. Vignes-Adler. 1998 Dynamics of real three dimensional foams. *Phys. Rev. Lett.* **80**:5228–5231.
- [4] A.M. Kraynik, D.A. Reinelt and F. vanSwol. 2004 The structure of random polydisperse foam. *Phys. Rev. Lett.* **93**:208301.
- [5] G. Debregeas, H. Tabuteau and J.M. di Meglio. 2001 Deformation and flow of a two-dimensional foam under continuous shear. *Phys. Rev. Lett.* **87**:178305.

- [6] J. Lauridsen, M. Twardos and M. Dennin. 2002 Shear-induced stress relaxation in a two-dimensional wet foam. *Phys. Rev. Lett.* **89**:098303.
- [7] B. Dollet, F. Elias, C. Quilliet, C. Raufaste, M. Aubuoy and F. Graner. 2005 Two-dimensional flow of foam around an obstacle: Force measurements. *Phys. Rev. E* **71**:031403.
- [8] W. Drenckhan, S.J. Cox, G. Delaney, H. Holste and D. Weaire. 2005 Rheology of ordered foams – on the way to Discrete Microfluidics. *Coll. Surf. A* **263**:52–64.
- [9] C. Quilliet, M.A.P. Idiart, B. Dollet, L. Berthier and A. Yekini. 2005 Bubbles in sheared two-dimensional foams. *Coll. Surf. A* **263**:95–100.
- [10] F. Graner, Y. Jiang, E. Janiaud and C. Flament. 2001 Equilibrium states and ground state of two-dimensional fluid foams. *Phys. Rev. E* **63**:011402.
- [11] M. Asipauskas, M. Aubuoy, J.A. Glazier, F. Graner and Y. Jiang. 2003 A texture tensor to quantify deformations: the example of two-dimensional flowing foams. *Granular Matter* **5**:71–74.
- [12] D. Weaire and J.P. Kermode. 1983 Computer simulation of a two-dimensional soap froth I. Method and motivation. *Phil. Mag. B* **48**:245–249.
- [13] T. Okuzono and K. Kawasaki. 1995 Intermittent flow behavior of random foams: A computer experiment on foam rheology. *Phys. Rev. E* **51**:1246–1253.
- [14] I. Cantat and R. Delannay. 2003 Dynamical transition induced by large bubbles in two-dimensional foam flows. *Phys. Rev. E* **67**:031501.
- [15] N. Kern, D. Weaire, A. Martin, S. Hutzler and S.J. Cox. 2004 Two-dimensional viscous froth model for foam dynamics. *Phys. Rev. E* **70**:041411.
- [16] J.A.F. Plateau. 1873 *Statique Expérimentale et Théorique des Liquides Soumis aux Seules Forces Moléculaires*. Gauthier-Villars, Paris.
- [17] J.E. Taylor. 1976 The structure of singularities in soap-bubble-like and soap-film-like minimal surfaces. *Ann. Math.* **103**:489–539.
- [18] K. Brakke. 1992 The Surface Evolver. *Exp. Math.* **1**:141–165.
- [19] D. Weaire and N. Rivier. 1984 Soap, cells and statistics—random patterns in two dimensions. *Contemp. Phys.* **25**:59–99.
- [20] S. Hutzler, D. Weaire and F. Bolton. 1995 The effects of Plateau borders in the two-dimensional soap froth .III. Further results. *Phil. Mag. B* **71**:277–289.
- [21] D. Weaire. 1999 The equilibrium structure of soap froths: inversion and dec-

oration. *Phil. Mag. Lett.* **79**:491–495.

- [22] P.I.C. Teixeira, F. Graner and M.A. Fortes. 2002 Mixing and sorting of bidisperse two-dimensional bubbles. *Eur. Phys. J. E* **9**:161–169.
- [23] R.L. Fullman 1952 *Boundary Migration During Grain Growth* pp. 179–207. American Society for Metals, Cleveland.

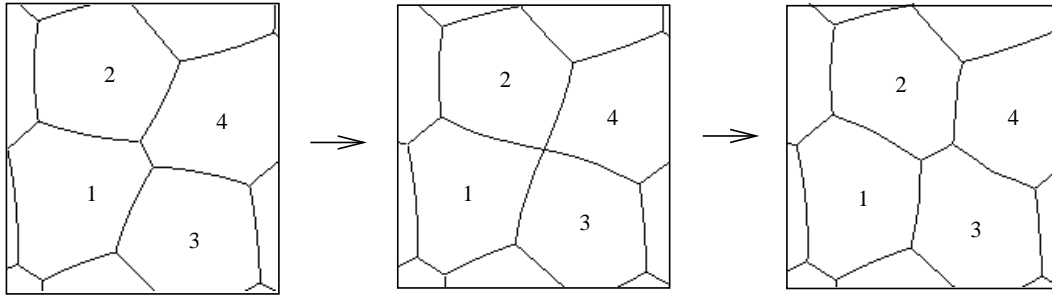


Fig. 1. A 2D foam minimizes its total perimeter, subject to the constraints imposed by bubbles of fixed area. At equilibrium, the foam consists of circular arcs that meet three-fold at  $120^\circ$ . As a flowing foam moves from one configuration to another, the changes in topology occur when a film shrinks to zero length and reforms with different neighbours. These T1 transformations result in a reduction in the foam's total energy, or, equivalently, its total perimeter.

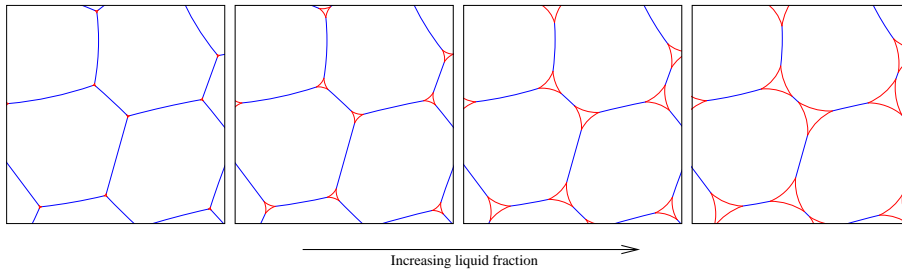


Fig. 2. A dry 2D foam can be decorated with a triangular Plateau border at each of the three-fold vertices to represent a wet system. The liquid fraction, which is defined as the liquid area divided by the total area, plays an important role in the foam's properties. To model the effects of liquid fraction, a cut-off length is introduced into the dry foam model, which allows T1s to be triggered when the vertex separation represents the point at which two Plateau borders touch.

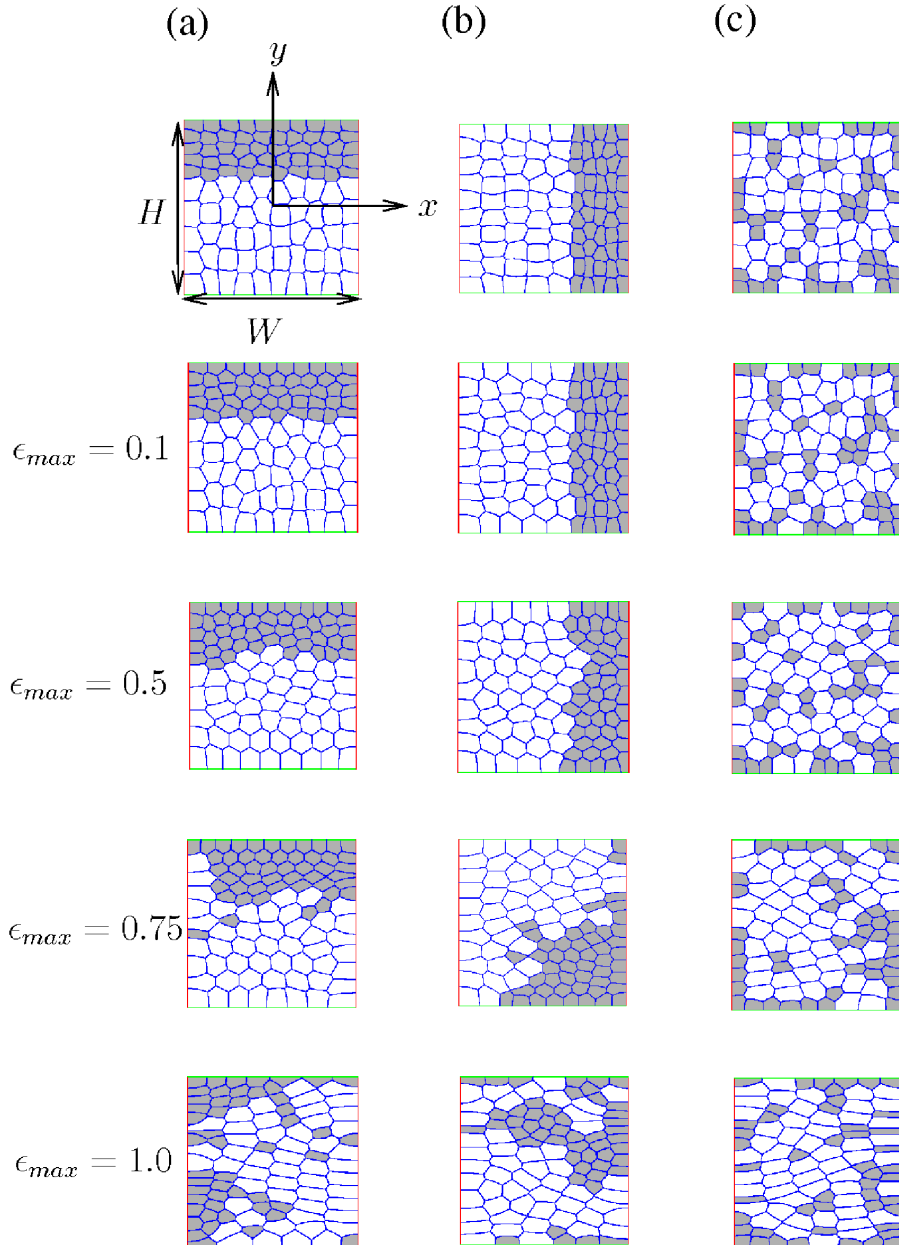


Fig. 3. The three bidisperse foams used to investigate mixing and the coordinate system. The small bubbles have been shaded for clarity. (a) Foam 1 starts with all large bubbles at the bottom of the foam. (b) Foam 2 starts with all large bubbles to one side of the foam. (c) Foam 3 is a random distribution of the two bubble areas. The first row shows the initial configuration. The second, third and fourth rows show, respectively, the result of 5 cycles of extensional shear with maximum strains of  $\epsilon_{max} = 0.1, 0.5, 0.75$  and  $1.0$ . For foams 1 and 2, there is evidently mixing; no sorting is observed for foam 3. After experiencing high strain amplitudes, these dry foams show bubbles which are elongated in the direction in which  $W$  is increasing.

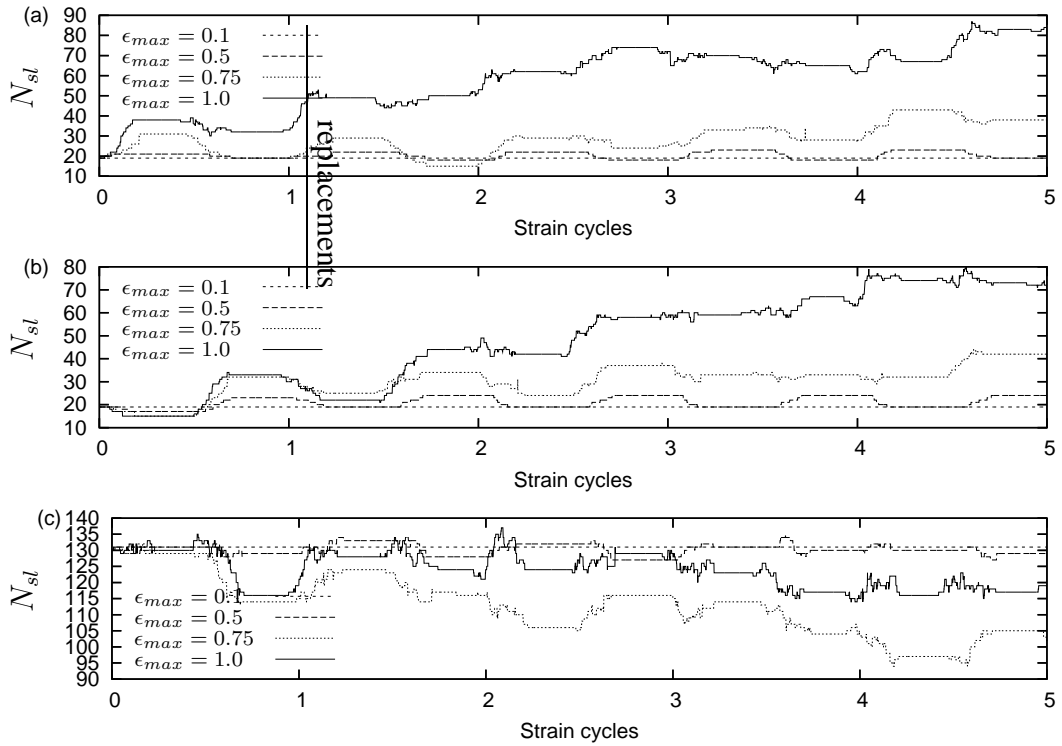


Fig. 4. The number of films separating large from small bubbles,  $N_{sl}$ , for each of the simulations illustrated in figure 3: (a) foam 1; (b) foam 2; (c) foam 3. Only in foams 1 and 2, where large and small bubbles are initially segregated, and only at high maximum strains ( $\epsilon_{max} = 1.0$ ), is there any significant mixing.  $N_{sl}$  decreases slightly for foam 3, perhaps indicating that there is a small amount of sorting in this initially mixed foam.

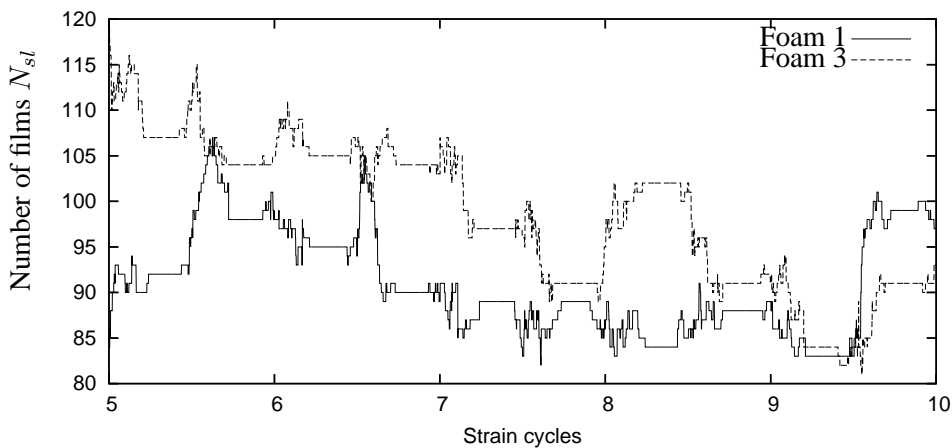


Fig. 5. The number of films separating large from small bubbles,  $N_{sl}$ , increases for foam 1 and decreases slightly for foam 3, which was initially unsorted, until the two are commensurate.

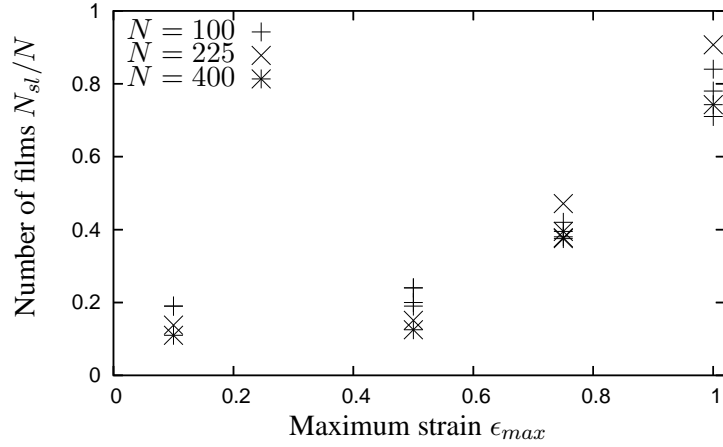


Fig. 6. The number of films separating large from small bubbles,  $N_{sl}$ , scaled by the number of bubbles  $N$ , after five strain cycles for foams 1 and 2.  $N_{sl}/N$  increases with maximum strain amplitude in the same way for foams of all sizes, justifying the use throughout of  $N = 100$ .

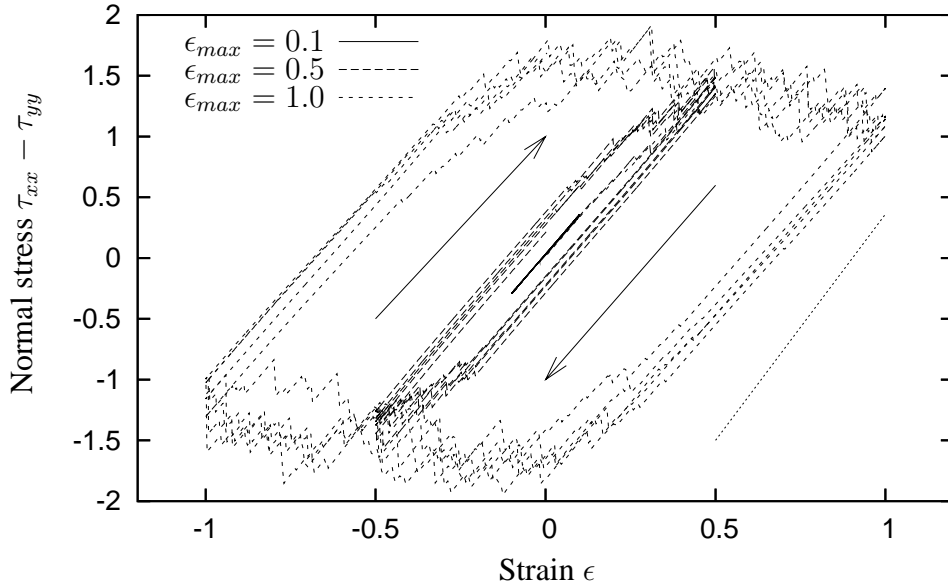


Fig. 7. The shear modulus of a 2D foam, in this case foam 1, does not vary greatly from the value for a honeycomb (bottom right), even when highly disordered. Stress-strain curves are shown for all three values of  $\epsilon_{max}$ . Arrows indicate the orientation of the cycle; the area inside each curve is the energy dissipated in each cycle, which is greater for higher strain amplitudes. All three curves commence at the origin.

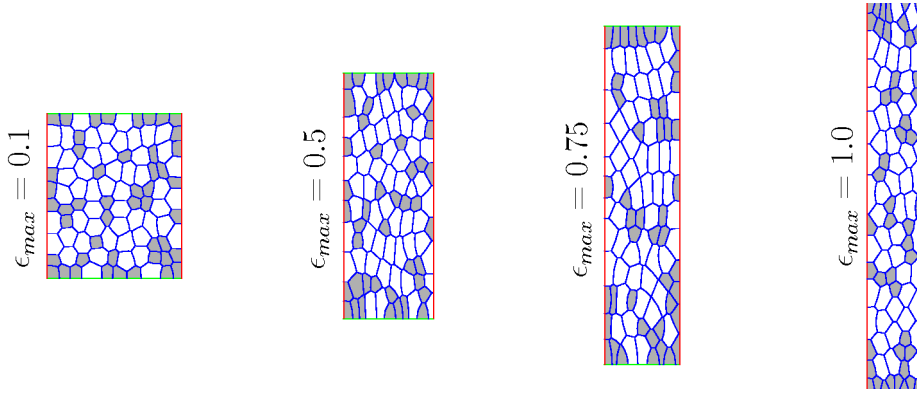
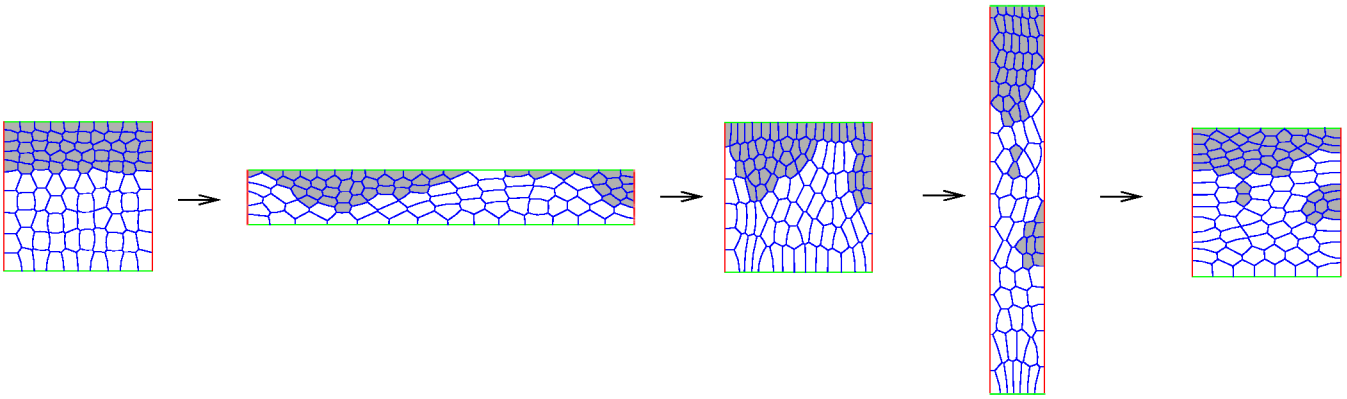


Fig. 8. Images of the foam at maximum extension, in the case of an initially mixed foam (Foam 3). With  $\epsilon_{max} = 1.0$ , the foam is only about 5 bubbles across at this point.

(a)



(b)

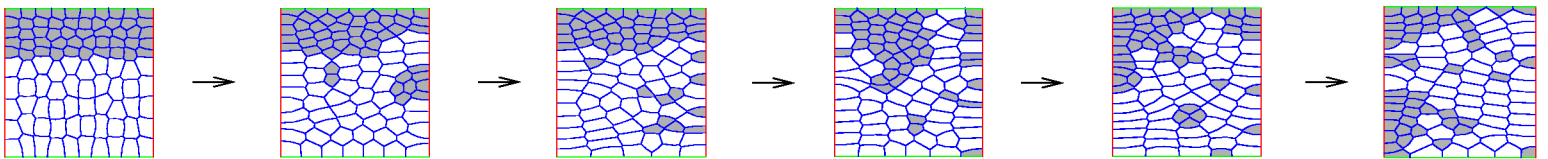


Fig. 9. Images of Foam 1, with all the large bubbles initially at the bottom of the foam, for  $\epsilon_{max} = 1.0$ . (a) The first cycle at  $t = 0, \pi/2, \pi, 3\pi/2$  and  $2\pi$ ; first  $W$  increases to its maximum value, then  $H$  does the same. (b) The configuration of Foam 1 after each full cycle (i.e. at  $t = 0, 2\pi, 4\pi, \dots$ ). The mixing of the two bubble sizes occurs incrementally, with a few small bubbles being pushed between the larger ones in each cycle.

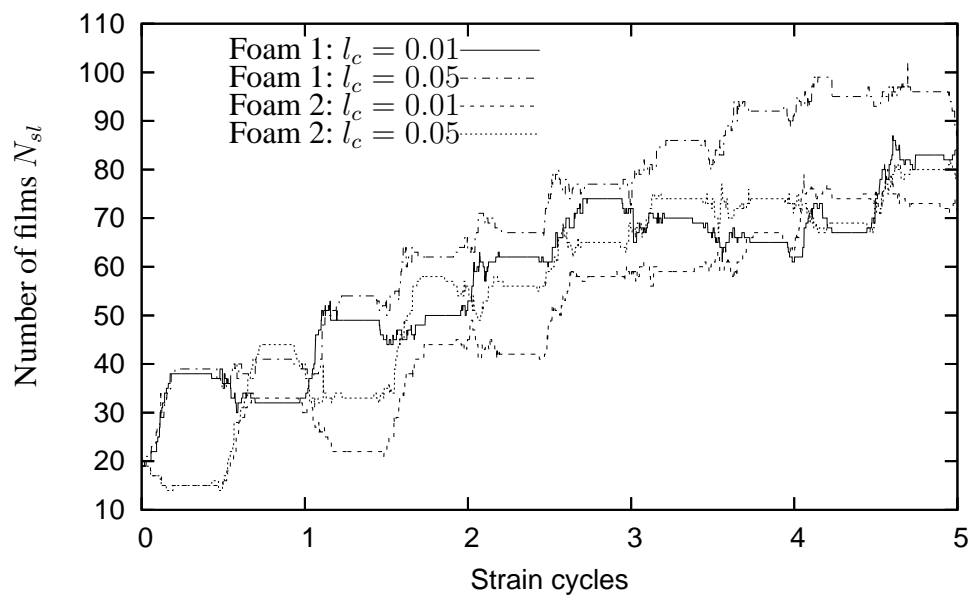


Fig. 10. Increasing the liquid fraction by a factor of 25 means that mixing occurs more rapidly for both foams 1 and 2 with a value of  $\epsilon_{max} = 1.0$ .